



## Self-assembly of the second-generation of nitroaryl-ended dendrons onto carbon



E.D. Farías<sup>a</sup>, J.I. Paez<sup>b,1</sup>, M.C. Strumia<sup>b</sup>, A.M. Baruzzi<sup>a</sup>, M.C.G. Passeggi (Jr.)<sup>c,d</sup>, V. Brunetti<sup>a,\*</sup>

<sup>a</sup> Departamento de Fisicoquímica (INFIQC, CONICET-UNC), Facultad de Ciencias Químicas, Universidad Nacional de Córdoba, Córdoba, Argentina

<sup>b</sup> Departamento de Química Orgánica (IMBIV, CONICET-UNC), Facultad de Ciencias Químicas, Universidad Nacional de Córdoba, Córdoba, Argentina

<sup>c</sup> Laboratorio de Superficies e Interfaces (IFIS, CONICET-UNL), Universidad Nacional del Litoral, Santa Fe, Argentina

<sup>d</sup> Departamento de Materiales, Facultad de Ingeniería Química, Universidad Nacional del Litoral, Santa Fe, Argentina

### ARTICLE INFO

#### Article history:

Received 21 December 2013

Received in revised form 17 February 2014

Accepted 6 April 2014

Available online 28 April 2014

#### Keywords:

second-generation dendron  
self-assembly  
glassy carbon electrodes  
dendronized electrodes  
Frumkin adsorption.

### ABSTRACT

We report the self-assembly of the second-generation of nitroaryl-ended dendrons onto carbon surfaces. The immobilized layer was characterized by cyclic voltammetry (CV), electrochemical impedance spectroscopy and atomic force microscopy (AFM). The response was analyzed in comparison to the first-generation dendron behavior. Reduction of both layers generates the hydroxylamine product. The resulting redox-active layer exhibits a well-behaved redox response for the adsorbed nitroso/hydroxylamine couple. The thermodynamic of the adsorption of both dendrons on glassy carbon electrodes was also studied by CV. The Frumkin adsorption isotherm was the best to describe the specific interactions. The AFM images showed a network film formation with embedded aggregates that completely covered the carbon surface. The average height suggests a tilted preferential adsorption for both molecules.

© 2014 Elsevier Ltd. All rights reserved.

### 1. Introduction

Carbon electrodes are widely used in electrochemical techniques due to their relatively low cost compared to other electrodes such as gold or platinum. However, electron transfer rates observed on carbon surfaces are often lower than those observed on metal electrodes[1]. In particular, the glassy carbon electrodes (GCE) constitute a very good alternative due to its excellent mechanical and electrical properties. GCE are relatively reproducible, chemically inert, and mostly used in a wide potential window. In addition, the carbon surface modification is relevant in the area of electrochemistry and materials science as it is a promising way for a rapid construction of new materials for electrocatalysis and (bio)sensor platforms. Generally, the carbon electrode derivatization is carried out following one of the subsequent strategies. First, through covalent modification of the electrode, for example

using oxidized groups (like carboxylic acids) located on the surface of carbon that yields anchoring groups to which the modifiers are connected. In particular, the electrochemical reduction of aryl diazonium salts is a well-established method whereby aromatic organic layers can be covalently tethered to carbon surfaces[2–8]. Second, some electrodes such as carbon paste ones can be doped with species mechanically immobilized during preparation[9–12]. Lastly, by physical adsorption of molecules on the substrates modified via supramolecular interactions. It is also well known that when considering immobilization via self-assembly of aromatic molecules on the electrode surface, the presence of functional groups may greatly affect the nature and magnitude of such interaction. Particularly, Wuest et al. recently reported that the adsorption energy of 1,3,5-trinitrobenzene onto carbon surfaces is about three times larger than for nitrobenzene molecules, and that the presence of carboxyl groups on the aromatic ring greatly increases the surface binding on graphite[13].

The aryl-nitro derivatives confined to an electrode surface are well-known redox mediators which exhibit high catalytic activity in the electrooxidation of reduced nicotinamide coenzyme (NADH)[14], and also have been successfully exploited for electrochemical detection of thiols[15]. In general, the aryl-nitro derivative, which is in fact precursor of the real mediator, is electrochemically transformed into the corresponding hydroxylamine

\* Corresponding author. INFIQC, Departamento de Fisicoquímica, Facultad de Ciencias Químicas, Universidad Nacional de Córdoba, Medina Allende y Haya de la Torre, Ciudad Universitaria, 5016 Córdoba, Argentina. Tel.: +54-351-5353850 ext 53487.

E-mail address: [verobrunetti@gmail.com](mailto:verobrunetti@gmail.com) (V. Brunetti).

<sup>1</sup> Max Planck Institute for Polymer Research, Mainz, Germany.

compound and then, the reversible two-electron oxidation of the hydroxylamine group leads to the nitroso group, which is the catalytically active compound. Several immobilization strategies have been developed for covalent modification of carbon surfaces with nitrophenyl groups, highlighting among them two methods: via spontaneous attachment of the nitrobenzenediazonium salt[16–18] and via self-assembly of nitrothiophenol[19]. The main advantage of both methods is that spontaneous grafting can take place with no electrochemical induction by simple immersing the substrate into a solution of either a diazonium salt or a proper thiol. However, the reactivity of the head group complicates the synthesis of some new aryl diazonium salts and only single component layers have been fabricated[20].

Dendrons are well-defined and highly branched molecules that are of great interest as new materials in many important application areas. They represent a structural component of the parent dendrimer, are also monodisperse, and even more, they are a wedged-shaped section of a dendrimer[21,22]. Dendrons can be used as building blocks to form a molecular self-assembly or adlayer on electrode surfaces. Thus, a common approach to amplify the effective area and quantity of functional groups onto an electrode is to graft dendritic molecules. On account of their controllable geometry, size, and functionality, dendrons rule interest for enlargement of active surfaces; however targeted control of surface architectures requires an understanding of dendron/dendron and dendron/surface interactions, as well as an in-depth knowledge of the structure of the dendrons in the solid state. Dendronization is a synthetic methodology that offers important advantages. The products which are obtained by means of it, present new and specific properties and are called dendronized materials[23].

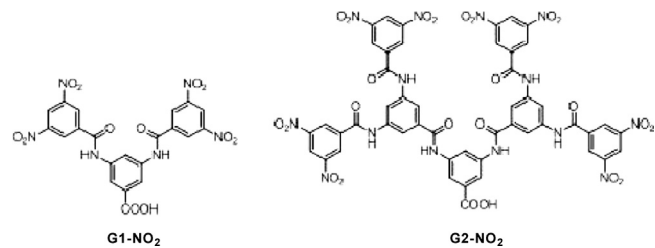
Self-assembly via physical adsorption is a particularly simple way of creating a film onto a surface. It needs neither preformation of oriented films nor special equipments. Physical adsorption is the result of relatively weak Van der Waal's interaction forces, a physical attraction between the electrode surface and the adsorbate. Hence, the method causes little or non-conformational changes of the dendritic molecule, and can be both simple and cheap. Under proper conditions, physical adsorption can result in adsorbed molecules forming multiple layers. However, it has the disadvantage that the adsorbed molecules may detach from the surface due to the weak binding forces[23].

In this paper, we report the self-assembly of the second-generation of nitroaryl-ended dendrons (G2-NO<sub>2</sub>) onto carbon surfaces and its comparison to the first-generation dendron behavior (G1-NO<sub>2</sub>). The self-assembling process of these adsorbate molecules were monitored by cyclic voltammetry (CV), electrochemical impedance spectroscopy (EIS) and atomic force microscopy (AFM). In this way, we report a powerful and versatile modification process, which can be applied to carbon materials without any conductivity or pretreatment requirements that generates promising platforms for electrocatalysis and sensor development.

## 2. Experimental

### 2.1. Materials

The synthesis of dendrons (**Scheme 1**) was obtained following the Kakimoto's procedure[24] (see S1 in the Supplementary Material). The rest of chemicals used within these experiments were reagent grade commercially available chemicals and were used without further purification. All solutions were prepared immediately prior to their use. Phosphate buffer solutions (PBS) used in this work contain Na<sub>2</sub>HPO<sub>4</sub>/NaH<sub>2</sub>PO<sub>4</sub>. Deionized water was used after purification in a Millipore Milli Q system and the actual pH



**Scheme 1.** Schematic representation of both dendrons: G1-NO<sub>2</sub> and G2-NO<sub>2</sub>.

of the solutions was determined with a Hanna Instruments pH/ion analyzer model 209.

### 2.2. Glassy carbon electrodes preparation

Prior to its modification, the glassy carbon electrodes (GCE) (CH Instruments, Inc. Austin, TX) of 3.0 mm diameter were polished using 1, 0.3 and 0.05 μm alumina (Buehler) and rinsed with water and ethanol. After its polishing, the electrodes were sonicated for 1 minute in distilled water and dried in a N<sub>2</sub> flux. GCE were incubated in a Dimethylsulfoxide (DMSO) solution containing either G1-NO<sub>2</sub> or G2-NO<sub>2</sub> for different times and concentrations. After the modification, the derivatized surface was subsequently rinsed with copious volumes of ethanol and water, and employed immediately after its preparation.

### 2.3. Electrochemical measurements

All electrochemical measurements were performed at room temperature with a CH Instruments Multipurpose Electrochemical Analyzer. A conventional three-electrode system, comprising a glassy carbon working one, a platinum foil as the auxiliary, and a Ag/AgCl 3.0 M NaCl electrode (from Bioanalytical Systems, Inc.) as the reference, was used for all measurements. All potentials were reported versus the Ag/AgCl reference electrode at room temperature. Nitrogen gas was used to deaerate all aqueous solutions before their use. If not otherwise mentioned, scans were started at the positive end of the potential range in cyclic voltammetry (CV). The impedance data were analyzed by non-linear least square fits using the Zview software[25]. A sinusoidal potential modulation of 10 mV amplitude was superimposed on a fixed d.c. potential and the amplitude and phase angle of the resulting current were recorded at frequencies ranging from 1 × 10<sup>-5</sup>–100 kHz.

### 2.4. Atomic Force Microscopy (AFM)

AFM images were acquired with a commercial Nanotec Electronic System operating in tapping-mode at an atmosphere pressure and room temperature. Acquisition and image processing were performed using the WS × M free software[26]. V-shaped Olympus RC800PSA cantilevers (Olympus Corporation, Tokyo, Japan) made of silicon nitrite coated with Au/Cr (resonance frequency in the range of 70–90 kHz, nominal spring constant in the range of 0.05–0.1 N/m and a radius of curvature less than 20 nm) were used. The samples for AFM analysis were prepared by immersing freshly cleaved highly oriented pyrolytic graphite (HOPG) in a DMSO solution containing 1 mM of either G1-NO<sub>2</sub> or G2-NO<sub>2</sub> for different reported times. Samples were subsequently rinsed with copious volumes of ethanol and water, dried under nitrogen flux and analyzed immediately.

### 3. Results and Discussion

#### 3.1. Electrochemical behavior

The spontaneous adsorption of G2-NO<sub>2</sub> onto GCE was followed by cyclic voltammetry (CV). Fig. 1a shows the representative cyclic voltammograms recorded from -0.8 to 0.5 V versus Ag/AgCl for a G2-NO<sub>2</sub> modified GCE in phosphate buffer solution (pH 7) at 0.1 Vs<sup>-1</sup>. The initial potential was set at 0.5 V. In the reductive direction, two large reduction waves labeled as I are observed at -0.446 V and -0.574 V. Two oxidative waves labeled as II, which appear only if the cathodic switching potential reaches -0.8 V, are observed at more positive potential values, -0.031 and 0.049 V. Once the oxidative processes appear, the corresponding reduction peaks appear at 0.020 and -0.080 V, respectively. This is indicative that I is electrochemically irreversible and that the new process, labeled as II, is electrochemically quasi-reversible. As expected the electrochemical behavior of G2-NO<sub>2</sub> adsorbed onto GCE is similar to that previously reported for G1-NO<sub>2</sub>[27], taking account that the voltammetry behavior is indeed characteristic of the electrochemical reduction of 3,5-dinitroaryl derivatives and it is consistent with the general mechanism previously described[28,29]. I corresponds to the four-electron reduction of each nitro moiety to the correlative aryl hydroxylamine (Ar-NHOH). On the subsequent positive-going sweep, II can be attributed to the two-electron oxidation/reduction of the aryl-hydroxylamine/aryl-nitroso (Ar-NO) moieties (See S2 in the Supplementary Material).

The voltammograms obtained for the modified electrodes are shown at various scan rates ( $v = 0.020\text{--}1.000\text{ Vs}^{-1}$ ) in Fig. 1b. The observation of well defined and persistent cyclic voltammetric peaks is indicative of a fairly stable Ar-NO/Ar-NHOH couple. The CV current decreases slightly after each cycle, showing a signal reduction of circa 30% after 40 cycles (See S3 in the Supplementary Material). A rapid decrease of oxidation peak current, which is registered by the increase of potential cycle number was recently reported for other nitroaromatic compounds[30] and have been attributed to the formation of relatively dense layer electrografted onto glassy carbon. It is worthy to point out that the electrochemical

signal of Ar-NHOH/Ar-NO groups does not disappear even after 5 minutes of ultrasonic cleaning of the modified electrode in DMSO, confirming the strong attachment between the physisorbed layer and the carbon surface. It is observed that the redox current peaks increase linearly with scan rates (Fig. 1c), indicating that redox waves are originated from the surface confined molecules. In addition, the formal potential [ $E^{0'} = (E_{ap} + E_{cp})$  where  $E_{ap}$  is the anodic peak potential and  $E_{cp}$  is the cathodic peak potential] is almost independent of the scan rate at values lower than 0.200 Vs<sup>-1</sup> suggesting a facile charge transfer kinetic over this range of scan rates (Fig. 1d).

The analysis of the electrochemical signal on CVs provides information about the density of the attached layer. Thus, the coulometric integration of the signal provides an estimation of the attached layer surface concentration. From the electrochemical characterization, the charge of electroactive species could be measured. The values for the surface concentration ( $\Gamma$ ) of Ar-NO<sub>2</sub> groups, given on mol cm<sup>-2</sup> were obtained from the integrated charges (Q) of the anodic peaks as follows[31]:  $\Gamma = Q/(nFS)$  where Q is the charge obtained from the area under the anodic peaks of system II after a baseline correction was done, n is the number of electrons exchanged per reactant molecule (n = 2), F is the faraday constant and S represents the area of the electrode. The results were not corrected by surface roughness, which was assumed constant. Fig. 2 shows the surface concentration of -NO<sub>2</sub> groups adsorbed on GCE incubated in a 0.3 mM solution of G1 and G2/DMSO as a function of the dipping time ( $t_{acc}$ ). Initially, the surface concentration grows up to reach a plateau in a short time at a value of circa 0.9 nmol/cm<sup>2</sup> for both dendrons. For comparison purposes, 1.2 nmol/cm<sup>2</sup> is the value reported previously for a monolayer of 4-nitrothiophenol covalent attached to carbon[19]. It is worthy of mention that the surface concentration is related to the quantity of nitro moieties and G2-NO<sub>2</sub> has the double of -NO<sub>2</sub> groups than G1-NO<sub>2</sub>. The inset of Fig. 2 displays a zoom region at short times, which shows a linear response for the incorporation of peripheral -NO<sub>2</sub> groups onto the electrode surface for both dendrons. It is clearly shown that G2-NO<sub>2</sub> contributes faster than G1-NO<sub>2</sub> to the electrode surface modification, finding a relation of 3/1 (greater than the expected relation of 2/1) between the slopes. In relation to the number of surface-bound Ar-NO<sub>2</sub> groups that have been determined, it is worth stressing that

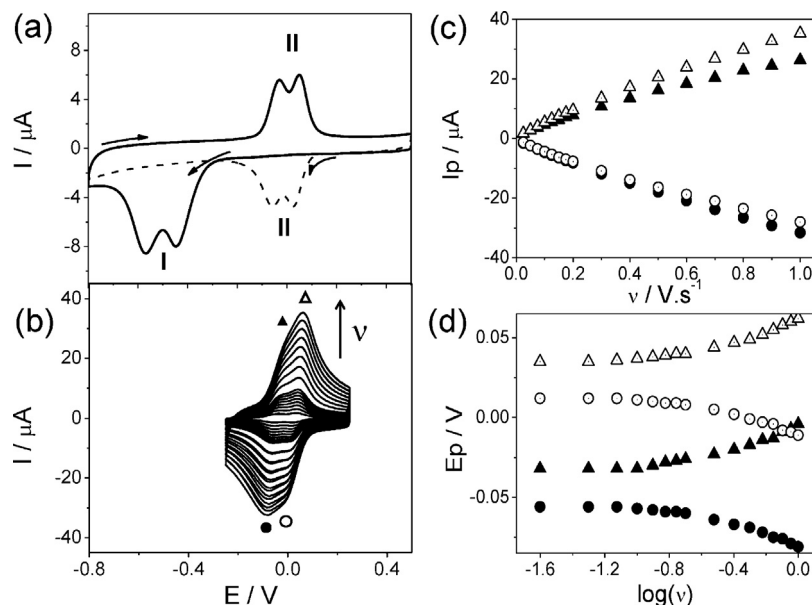


**Fig. 1.** (a) Cyclic voltammograms for G2-NO<sub>2</sub>/GCE in 0.1 M PBS (pH 7) at 0.1 Vs<sup>-1</sup>: first (solid line) and second (dashed line) scans. (b) Cyclic voltammograms at different sweep rates measured in the potential range from -0.3 to 0.3 V. (c) Plots of the anodic and cathodic peak current as a function of scan rate from (b). (d) Plots of the peak potential as a function of log v obtained from (b).

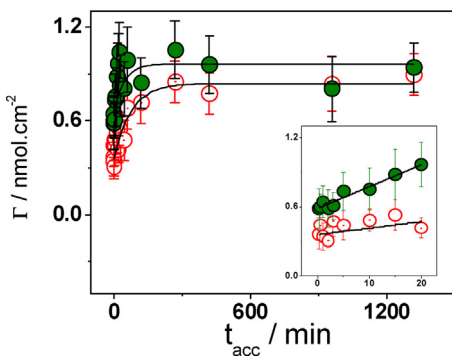


**Fig. 2.** Surface coverage of aryl-nitro groups on GCE as a function of the incubation time ( $t_{acc}$ ) in a 0.3 mM solution of G1-NO<sub>2</sub>/DMSO (○) and G2-NO<sub>2</sub>/DMSO (●). Inset: zoom at low  $t_{acc}$ .

only electroactive surface groups can be detected by these methods. Under this work conditions, the reduction of surface Ar-NO<sub>2</sub> groups is chemically irreversible and hence site-to-site electron hopping cannot be a mechanism for charge transfer from the electrode to the outer parts of a multilayer film[32]. Thus, it is possible that some Ar-NO<sub>2</sub> groups are relatively far from the surface for which electron tunneling is very inefficient leading to groups that are electroinactive and are not detected voltammetrically[32].

To gain insight about the immobilization process of these dendrons onto carbon, we have examined the isotherms and energetic adsorption. A plot of the maximum value of surface concentration ( $\Gamma_{max}$ ) versus dendron concentration ( $C_{dendron}$ ) is shown in Fig. 3a. The surface concentration grows rapidly at low  $C_{dendron}$  and then asymptotically approaches the limiting surface concentration value. As well, we have studied the adsorption isotherm derived from the dependence between  $C_{dendron}$  and the fractional coverage of the electrode surface ( $\theta$ ). The surface coverage was defined as  $\theta = \Gamma/\Gamma_{max}$  from cyclic voltammograms obtained at a given  $t_{acc}$  for different  $C_{dendron}$ . Fits of different adsorption isotherm models (Langmuir, Frumkin, Temkin and Freundlich) were tested to describe the adsorption of each dendron on GCE. The best fits were obtained with the Frumkin adsorption isotherm[33], which is:  $\beta C_{dendron} = \theta/(1-\theta) * \exp(-g'\theta)$ , where  $\beta$  is the adsorption coefficient, which expresses the strength of adsorption and  $g'$  is a parameter which characterizes the interaction between the adsorbed species. If  $g' > 0$ , the adsorbed molecules are attracted

one to each other and at this time, the adsorption rate is faster than for those adsorbed molecules which did not interact. If  $g' < 0$ , the adsorbed molecules are excluded one another and herein, the adsorption rate is slower than for those adsorbed molecules which did not interact one another. A plot of  $\ln[\theta/C_{dendron}(1-\theta)]$  against  $\theta$ , called the linear form of Frumkin's isotherm (See S4 in the Supplementary Material), is shown in Fig. 3b and the fits are shown in solid line. For the best fits, the parameters were:  $\beta_{G1} = 1.05 \times 10^5 \text{ M}^{-1}$ ,  $\beta_{G2} = 13.3 \times 10^5 \text{ M}^{-1}$ ,  $g'_{G1} = -4.3$  and  $g'_{G2} = -4.6$  where 0.65 and 0.93 are the chi-square statistical parameter, respectively. There is an excellent agreement between experimental data and the results of the fits. The free energy of adsorption ( $\Delta G_{ads}$ ) can be determined from the adsorption coefficient:  $\beta = \exp(-\Delta G_{ads}/RT)$  where  $R$  is the gas constant and  $T$  is the absolute temperature. Values of  $\Delta G_{ads,G1} = -38.6 \text{ kJ mol}$  and  $\Delta G_{ads,G2} = -44.9 \text{ kJ mol}$  were obtained for the standard free adsorption energy of each dendron at 298 K. This is indicative that the overall adsorption processes of dendron molecules onto the GCE are energetically favorable. In addition, a negative value for  $g'$  indicates that there was a strong exclusion interaction among the adsorbed species on the electrode surface, similar to the reported behavior of thiol-derivatized porphyrin adsorption onto gold [34]. Negative values of the interaction parameter correspond to repulsion in the surface layer, i.e., diminishing capability for adsorption with increasing surface coverage and supporting the hypothesis of aggregation in the adsorption layer.[35]

The blocking properties of the layer-coated electrodes were evaluated using diffusion controlled redox couple as probes. Thus, the electron transfer kinetics of Ru(NH<sub>3</sub>)<sub>6</sub><sup>2+/3+</sup> and Fe(CN)<sub>6</sub><sup>3-/4-</sup> at dendronized GCE was also investigated. Figs. 4a and 4b depict the CVs obtained at the bare GCE, G1-NO<sub>2</sub>/GCE and G2-NO<sub>2</sub>/GCE dendronized electrodes obtained by incubation of GCE in a 1.0 mM dendron/DMSO solution during 15 minutes. The bare GCE shows a voltammogram for the corresponding redox couple associated to the reversible diffusion controlled electron transfer reactions. The electrochemical profile for the dendronized GCE exhibits an additional electrochemical process related to the Ar-NO/Ar-NHOH couple, and no significant differences were found in the electrochemical response of the redox probes at PBS pH = 7, indicating that the surface modification of the electrodes apparently do not block the electron transfer reaction of the redox probes at neutral pH. The electron transfer capability of the dendronized surfaces was further investigated by faradaic impedance spectra as shown

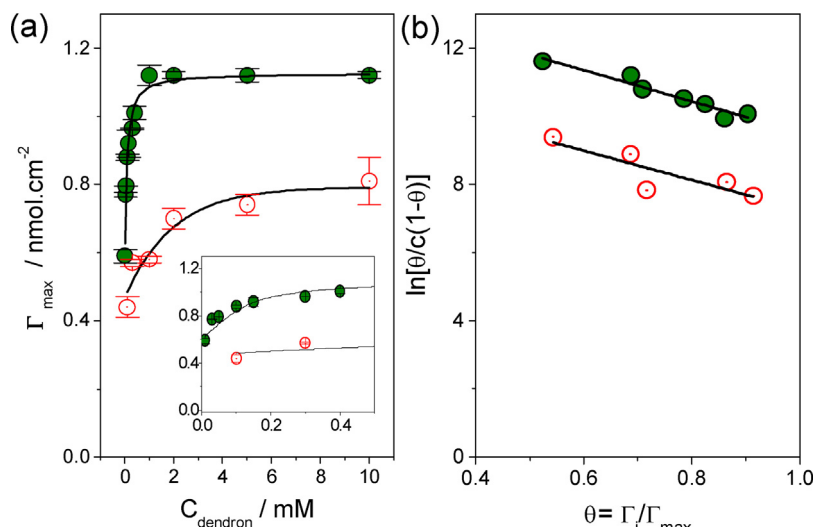


**Fig. 3.** (a) Surface coverage as a function of dendron concentration by dipping GCE in G1-NO<sub>2</sub>/DMSO (○) and G2-NO<sub>2</sub>/DMSO (●) solutions for 15 minutes. Inset: zoom at low  $C_{dendron}$ . (b) Plots of the linear form of Frumkin isotherms for G1-NO<sub>2</sub> (○) and G2-NO<sub>2</sub> (●) adsorption.

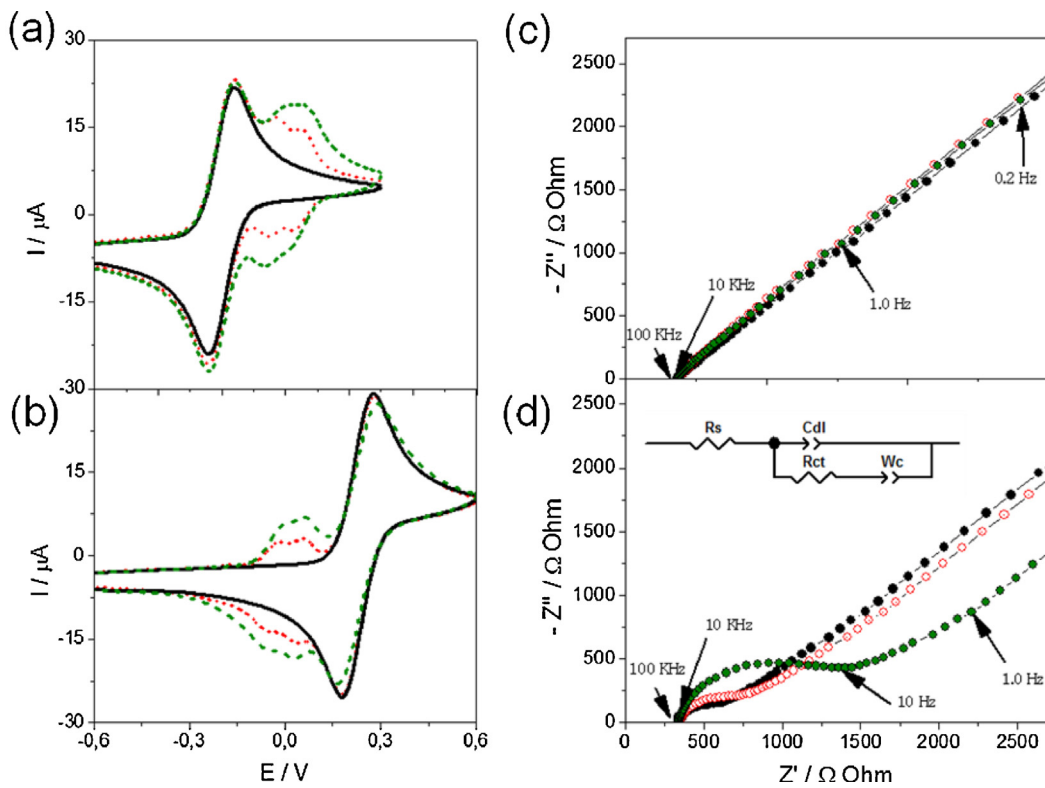


**Fig. 4.** Cyclic voltammograms for a GCE in 0.1 M PBS (pH 7) containing 2 mM Ru(NH<sub>3</sub>)<sub>6</sub>Cl<sub>3</sub> (a) or 2 mM K<sub>3</sub>Fe(CN)<sub>6</sub> (b) at 0.1 Vs<sup>-1</sup>. Bare GCE (solid line) and, GCE after the incubation in a 1 mM solution of G1-NO<sub>2</sub>/DMSO (dotted line) and G2-NO<sub>2</sub>/DMSO (dashed line) for 15 minutes. Corresponding Nyquist plots obtained for bare GCE (●) and, GCE after the incubation in G1-NO<sub>2</sub>/DMSO (○) and G2-NO<sub>2</sub>/DMSO (●) solutions in the positive (c) and negative (d) redox couples. Randles circuit model is depicted in the inset of (d).

in Figs. 4c and 4d. By fitting the Fe(CN)<sub>6</sub><sup>3-/4-</sup> data using the Randles equivalent circuit (inset of Fig. 4d) an increment of only 300 ohms was observed for G1 and 3 times greater for G2 (circa 900 ohms). These changes represent in both cases a very low increase of the charge transfer resistance ( $R_{ct}$ ). The adsorption kinetics can also be analyzed in terms of the  $R_{ct}$  changes of modified GCE in a 0.3 mM dendron solution after different incubation times. A good linear correlation between the increase in  $R_{ct}$  and  $\Gamma$  was found (See S5 in the Supplementary Material).

In addition, acid-base properties of the self-assembled layers have been studied by using electrochemical impedance spectroscopy with [Fe(CN)<sub>6</sub>]<sup>4-/3-</sup> as redox probe. Fig. 5 shows that the impedance for both dendronized GCEs is pH dependent. The titration curves of the impedance are plotted as a function of the pH solution for each dendron, as shown in the inset of Fig. 5. The  $R_{ct}$  versus the pH plots exhibit a sigmoidal shape indicating the applicability of  $R_{ct}$  to get information about the fractional degree of acidic or basic groups on the surface and, viewing the plots as direct titration curves[36]. The pH solution at which the  $R_{ct}$  (inset of Fig. 5) is midway between the almost stationary stages observed at high and low pH is 5, in agreement with the value reported by Damos et al. for 4-nitrothiophenol/4-mercaptopbenzoic acid binary self-assembled layer on gold[37]. This apparent surface p<sub>K<sub>a</sub></sub> value (the negative base-10 logarithm of the acid dissociation constant of the dendron) can be associated with many particular aspects of surface molecules, including strong intermolecular lateral hydrogen bonding between the surface molecules. Hydrogen bond formation causes the acidic protons to be held more tightly on the surface layer and deprotonation of an acid layer is energetically unfavorable because of the high electrostatic repulsion that the neighboring ionized carboxylate groups undergo at the interface[37]. For example, Saby et al. reported a shift of the p<sub>K<sub>a</sub></sub> of benzoic acid value

from 4.2 in solution to 2.8 when it is covalently attached onto glassy carbon, which they mentioned to be due to some specific interfacial effect between the carbon surface and carboxylate functionalities or the phenyl ring of the layer[38]. In this work, the p<sub>K<sub>a</sub></sub> values are more likely related to the fact that both functional groups (carboxylate and hydroxylamine) are available on the surface, which is indicative of a probably parallel orientation between the aromatic rings of each dendron body and the carbon surface, enhanced by  $\pi$  back-bonding interaction with the substrate.

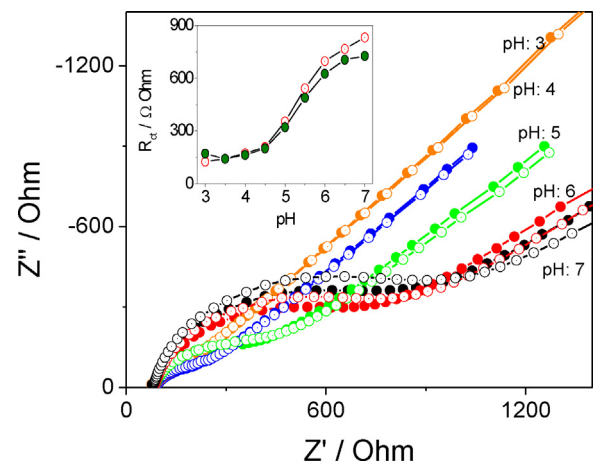


**Fig. 5.** Nyquist plots of G1-NO<sub>2</sub>/GCE (open circles) and G2-NO<sub>2</sub>/GCE (solid circles) in the presence of a 2 mM K<sub>3</sub>Fe(CN)<sub>6</sub> at different pH values in the range of 3 to 7. Inset: faradaic impedance titration plots for G1-NO<sub>2</sub>/GCE (○) and G2-NO<sub>2</sub>/GCE (●). Incubation conditions: 60 min, 0.3 mM.

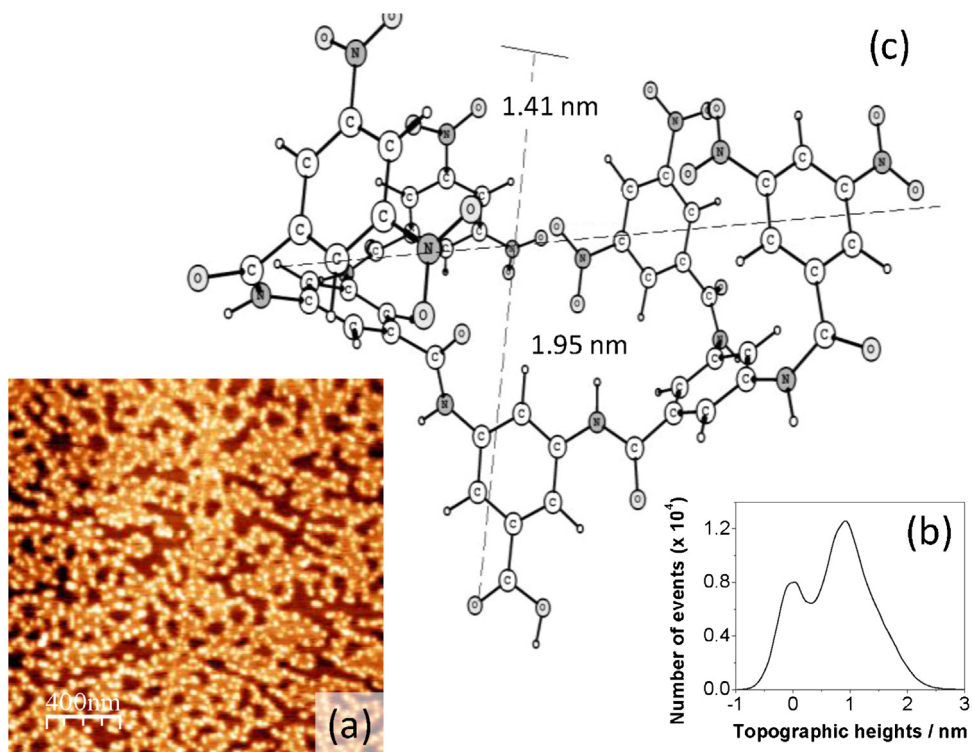


**Fig. 6.** (a) AFM topographical image ( $2000\text{ nm} \times 2000\text{ nm}$ ) of a modified HOPG surface incubated in a 1 mM G2-NO<sub>2</sub>/DMSO solution for 5 seconds. (b) Surface roughness profile. (c) Structure of G2-NO<sub>2</sub> optimized in vacuum.

### 3.2. AFM imaging of G1-NO<sub>2</sub> and G2-NO<sub>2</sub> immobilized onto carbon surfaces

The HOPG electrode was chosen as substrate for the AFM experiments due to the fact that small dendrons can only be correctly imaged by AFM when they are attached onto very smooth electrode surfaces. For comparison, the GCEs used in the electrochemical studies have a root-mean-square roughness (RMS) of about 2.0 nm while HOPG electrodes have RMS values of less than 0.2 nm. In addition, the electrochemical experiments done over HOPG electrodes presented (not shown here) a similar behavior as those obtained for GCE.

AFM measurements were carried out to study the dendron layers adsorbed on HOPG substrates in order to obtain topographical information, varying the incubation time and concentration of dendron solutions. Fig. 6a shows an AFM image of HOPG incubated in a 1 mM G2-NO<sub>2</sub>/DMSO solution for 5 seconds. Nanometer features due to dendrons adsorption are observed. They appear as clusters or dendron aggregates that nucleate in isolated regions. In tapping-mode, the low tip-sample interactions allow the reproducible and repetitive imaging of the same surface area without any apparent distortion. Surface roughness profile related to dendrons structure is plotted in Fig. 6b and the calculated molecular size using Gaussian is depicted in Fig. 6c. The G2-NO<sub>2</sub> height values are within a range of 0.5–2 nm assuming as zero the surface of the bare HOPG. This suggests different adsorption geometries, as well as different dendron-substrate interactions. Similar results were previously reported for the G1-NO<sub>2</sub> adsorption[39]. In the present case, the most probable value for G2-NO<sub>2</sub> was found to be circa 1.0 nm, instead of the lower value of 0.6 nm obtained for G1-NO<sub>2</sub>[39].

The presence of functional groups can significantly alter the nature and extent of interactions between dendrons and the surface. The occupied surface area may depend on the chemical

structure, steric interaction between dendrons, and rigidity of the molecule. Fig. 7 shows AFM images obtained for a HOPG substrate after dendron adsorption (G1-NO<sub>2</sub> or G2-NO<sub>2</sub>) at different incubation times (5 and 30 seconds). In the very beginning of processes, the G2-NO<sub>2</sub>/HOPG surface shows a sort of clusters or islands net array with an occupied area of 59% while the G1-NO<sub>2</sub>/HOPG surface seems to be in an earlier stage of the layer formation with only a 10% of covered area. For an incubation time of 30 seconds, the adsorption of G2-NO<sub>2</sub> onto HOPG reaches a coverage area of 90% while G1-NO<sub>2</sub>/HOPG exhibits a value close to 55%. The cooperative effect of the aromatic rings and the multifunctionality of dendrons (containing nitro and carboxylic groups) allow a quick and direct adsorption onto carbon surfaces. This effect is enhanced with increasing dendron generation. The analysis of the topography of the deposits, as a function of incubation time, indeed confirms that the aromatic rings cooperative effect is in fact depending on the dendron generation, possibly driven by the increasing number of aromatic rings (and nitro-ended groups) available to interact with the substrate at higher dendron generation. This result is in good agreement with the electrochemical results, which show a more than expected increment in the peak areas observed for G2-NO<sub>2</sub>/GCE (associated with the Ar-NO<sub>2</sub> groups) comparing to G1-NO<sub>2</sub>/GCE peaks, associated not only to the increase of the number of peripheral nitro groups but also the increase of the amount of immobilized species.

Fig. 8 depicts the AFM topographical images of carbon surfaces modified either by G1-NO<sub>2</sub> (a) and G2-NO<sub>2</sub> (b) after their immersion in a 1 mM dendron/DMSO solution for 15 minutes. In both cases, a completely dendron covered surface is obtained. Taking into account a cross section analysis based on the height profiles obtained along each image (Figs. 8c and 8d), we can conclude that G2-NO<sub>2</sub>/GCE exhibits a smoother surface than G1-NO<sub>2</sub>/GCE. The RMS values of dendronized surfaces are 0.56 nm for the first-generation dendron, while it reduces to 0.23 nm for

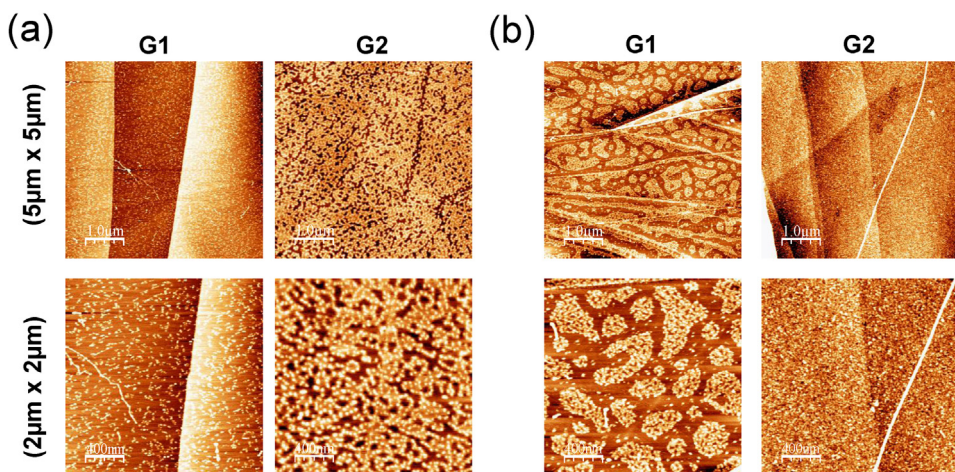


**Fig. 7.** AFM topographical images of modified HOPG surfaces incubated in a 1 mM of either G1-NO<sub>2</sub>/DMSO or G2-NO<sub>2</sub>/DMSO solutions for 5 (a) and 30 seconds (b).

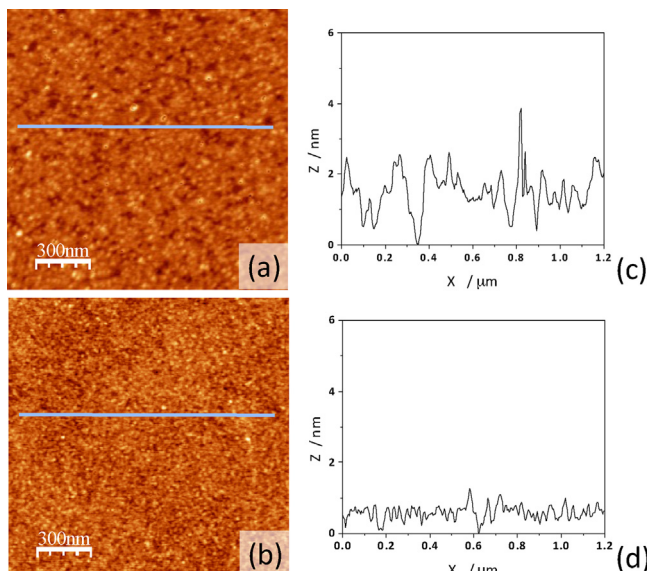


**Fig. 8.** AFM topographical images (1500 nm × 1500 nm) of modified HOPG surfaces incubated in a 1 mM of either G1-NO<sub>2</sub>/DMSO (a) or G2-NO<sub>2</sub>/DMSO (b) solutions for 15 minutes. Surface height profiles acquired along the AFM images shown in (a) and (b) are plotted in (c) and (d), respectively.

the second-generation one, which is indicative of the formation of a more compact layer in the last case.

#### 4. Conclusions

Two dendronized carbon surfaces were investigated after the self-assembly of the first and second-generation of nitroaryl-ended dendrons. The immobilized layer was characterized by cyclic voltammetry, electrochemical impedance spectroscopy and atomic force microscopy. The thermodynamic of the adsorption was interpreted using the Frumkin isotherm model, showing a negative value for the Frumkin coefficient related to the aggregation of the adsorbates. The AFM images confirm the formation of a network film with embedded aggregates that cover completely the carbon surfaces after a few minutes. The average heights suggest a tilted preferred adsorption for both molecules in the early stages of the film formation. The cooperative effect of the aromatic rings and the multifunctionality of dendrons allow a quick and direct adsorption

onto carbon surfaces, pointing out a noticeable increment of this effect with increasing dendron generation. In summary, we propose a simple way to modify carbon materials without any conductivity or pretreatment requirements, generating nitroaryl-ended platforms that exhibit a slight blocking to charge transfer reactions. Both dendronized carbon surfaces are promising candidates to be used in electrocatalysis and sensor developments.

#### Acknowledgements

We wish to express our gratitude to Diego Andrada for his valuable help with Gaussian calculations. Financial support from CONICET, ANPCyT, and SECYT-UNC is gratefully acknowledged. E.D.F. and J.I.P. thank CONICET for their fellowships.

#### Appendix A. Supplementary data

Supplementary material related to this article can be found, in the online version, at <http://dx.doi.org/10.1016/j.electacta.2014.04.029>.

#### References

- B. Uslu, S.A. Ozkan, Combinatorial Chemistry and High Throughput Screening 10 (2007) 495–513.
- S. Gam-Derouich, S. Mahouche-Chergui, M. Turmine, J.Y. Piquemal, D.B. Hassene-Chehimi, M. Omastovs, M.M. Chehimi, Surface Science 605 (2011) 1889–1899.
- A.L. Gui, G. Liu, M. Chockalingam, G. le Saux, E. Luais, J.B. Harper, J.J. Gooding, Electroanalysis 22 (2010) 1824–1830.
- M. Kullapere, F. Mirkhalaf, K. Tammeveski, Electrochimica Acta 56 (2010) 166–173.
- J. Lehr, B.E. Williamson, A.J. Downard, Journal of Physical Chemistry C 115 (2011) 6629–6634.
- G. Liu, J. Liu, T. Bocking, P.K. Eggers, J.J. Gooding, Chemical Physics 319 (2005) 136–146.
- L. Pilan, E.M. Ungureanu, G. Bidan, Nonlinear Optics Quantum Optics 39 (2009) 41–55.
- K.H. Vase, A.H. Holm, K. Norrman, S.U. Pedersen, K. Daasbjerg, Langmuir 23 (2007) 3786–3793.
- I. Svancara, K. Vytras, K. Kalcher, A. Walcarus, J. Wang, Electroanalysis 21 (2009) 7–28.
- I. Svancara, A. Walcarus, K. Kalcher, K. Vytras, Central European Journal of Chemistry 7 (2009) 598–656.
- D. Bellido-Milla, L.M. Cubillana-Aguilera, M. El Kaoutit, M.P. Hernandez-Artiga, J.L. Hidalgo-Hidalgo De Cisneros, I. Naranjo-Rodriguez, J.M. Palacios-Santander, Analytical and Bioanalytical Chemistry 405 (2013) 3525–3539.
- K. Vytras, I. Svancara, R. Metelka, Journal of the Serbian Chemical Society 74 (2009) 1021–1033.
- A. Rochefort, J.D. Wuest, Langmuir 25 (2009) 210–215.
- M. Santhiago, P.R. Lima, W.d.J.R. Santos, A.B.d. Oliveira, L.T. Kubota, Electrochimica Acta 54 (2009) 6609–6616.

- [15] P. Abiman, G.G. Wildgoose, R.G. Compton, *Electroanalysis* 19 (2007) 437–444.
- [16] C.G.R. Heald, G.G. Wildgoose, L. Jiang, T.G.J. Jones, R.G. Compton, *ChemPhysChem* 5 (2004) 1794–1799.
- [17] P. Abiman, G.G. Wildgoose, R.G. Compton, *Journal of Physical Organic Chemistry* 21 (2008) 433–439.
- [18] A.T. Masheter, G.G. Wildgoose, A. Crossley, J.H. Jones, R.G. Compton, *Journal of Materials Chemistry* 17 (2007) 3008–3014.
- [19] C. Médard, M. Morin, *Journal of Electroanalytical Chemistry* 632 (2009) 120–126.
- [20] M.M. Chehimi, *Aryl Diazonium Salts: New Coupling Agents and Surface Science*, Wiley, 2012.
- [21] G.R. Newkome, C.N. Moorefield, F. Vögtle, *Dendrimer Molecules: Concepts, Syntheses, Applications*, Wiley-VCH Verlag GmbH & Co. KGaA, Weinheim, Germany, 2002.
- [22] F. Vögtle, G. Richardt, N. Werner, *Dendrimer Chemistry: Concepts, Syntheses, Properties, Applications*, WILEY-VCH Verlag GmbH & Co. KGaA, Weinheim, Germany, 2009.
- [23] J.I. Paez, M. Martinelli, V. Brunetti, M.C. Strumia, *Polymers* 4 (2012) 355–395.
- [24] Y. Ishida, M. Jikei, M.A. Kakimoto, *Macromolecules* 33 (2000) 3202–3211.
- [25] ZView® software in, Scribner Associates.
- [26] I. Horcas, R. Fernandez, J.M. Gomez-Rodriguez, J. Colchero, J. Gomez-Herrero, A.M. Baro, *Review of Scientific Instruments* 78 (2007).
- [27] J.I. Paez, M.C. Strumia, M.C.G. Passeggi Jr., J. Ferron, A.M. Baruzzi, V. Brunetti, *Electrochimica Acta* 54 (2009) 4192–4197.
- [28] A.T. Masheter, L. Xiao, G.G. Wildgoose, A. Crossley, J.H. Jones, R.G. Compton, *Journal of Materials Chemistry* 17 (2007) 3515–3524.
- [29] G.G. Wildgoose, S.J. Wilkins, G.R. Williams, R.R. France, D.L. Carnahan, L. Jiang, T.G.J. Jones, R.G. Compton, *ChemPhysChem* 6 (2005) 352–362.
- [30] Y. Oztekin, Z. Yazicigil, A.O. Solak, Z. Ustundag, A. Okumus, Z. Kilic, A. Ramanaviciene, A. Ramanavicius, *Sensors and Actuators, B: Chemical* 166–167 (2012) 117–127.
- [31] A.J. Bard, L.R. Faulkner, *Electrochemical Methods*, Wiley, New York, 1980.
- [32] P.A. Brooksby, A.J. Downard, *Langmuir* 20 (2004) 5038–5045.
- [33] B.B. Damaskin, O.A. Petrii, *Adsorption of organic compounds at electrodes*, Plenum, New York, 1971.
- [34] G. Zuo, X. Liu, J. Yang, X. Li, X. Lu, *Journal of Electroanalytical Chemistry* 605 (2007) 81–88.
- [35] S. Karakashev, E. Manev, A. Nguyen, *Advances in Colloid and Interface Science* 112 (2004) 31–36.
- [36] T. De, F. Paulo, H.D. Abrúñ, I.C.N. Diogenes, *Langmuir* 28 (2012) 17825–17831.
- [37] D.D. Justino, A.L.A. Lage, D.E.P. Souto, J.V. Da Silva, W. Torres Pio Dos Santos, R. De Cássia Silva Luz, F.S. Damos, *Journal of Electroanalytical Chemistry* 703 (2013) 158–165.
- [38] C. Saby, B. Ortiz, G.Y. Champagne, D. Belanger, *Langmuir* 13 (1997) 6805–6813.
- [39] E.D. Farias, V. Brunetti, J.I. Paez, M.C. Strumia, M.C.G. Passeggi Jr., J. Ferron, *Microscopy and Microanalysis* 20 (2014) 61–65.